

# Inkjet Printing of Piezoelectric Lead Magnesium Niobate-Lead Titanate Thick Films

Andreas Rathjen<sup>1</sup>, Clemens Junker<sup>1</sup>, Hana Uršič<sup>2,3</sup>, Marija Kosec<sup>2,3</sup>, Klaus Krüger<sup>1</sup>

<sup>1</sup>Helmut Schmidt University/University of the Federal Armed Forces Hamburg  
Holstenhofweg 85, 22043 Hamburg, Germany  
andreas.rathjen@hsu-hh.de

<sup>2</sup>Electronic Ceramics Department, Jožef Stefan Institute  
Jamova 39, SI-1000 Ljubljana, Slovenia

<sup>3</sup>Centre of Excellence NAMASTE  
Jamova 39, SI-1000 Ljubljana, Slovenia

## Abstract

*This study shows the fabrication of lead magnesium niobate-lead titanate (PMN–PT) thick-films by inkjet printing on ceramic substrates for the first time. PMN–PT powder, prepared by mechanochemical synthesis, is dispersed in an organic solvent using a three roll mill to form a high-viscosity paste. For printing, the paste is thinned to a low-viscosity ink. Small amounts of ethyl cellulose in the ink prevent sedimentation. Glass particles are added to the paste to improve adhesion on the substrate surface. A two step inkjet-printing process forming homogeneous layers is introduced. After sintering at 950 °C for 2 h, piezoresponse force microscopy (PFM) is used to investigate the piezoelectric response of the printed films.*

Key words: Piezo Ceramics, PMN–PT, Inkjet-Printing, Digital Printing, Thick Film

## Introduction

The progress in thick-film technology is the result of the growing opportunities offered by miniaturized electromechanical systems. Thick-film structures can be multi-functional and can be used in a variety of applications, such as sensors, actuators and transducers.

Pb(Mg<sub>1/3</sub>Nb<sub>2/3</sub>)O<sub>3</sub>–PbTiO<sub>3</sub>-based materials (PMN–PT) are characterized by a high dielectric permittivity, promising piezoelectric properties [1–3] and a large electrostriction [4–6]. They are the active materials for applications such as sensors, actuators, ultrasonic medical diagnostics or underwater acoustics and active vibration control [7]. The morphotropic phase boundary (MPB) in this system is located close to the 0.65PMN–0.35PT composition.

Thick films are more cost efficient than bulk ceramics of the same composition, because they can be usually sintered at much lower temperature. However, a low sintering temperature also needs a very chemically homogeneous powder. The inferior

properties sometimes observed for thick films are very often related to the use of a powder that is only partly reacted. This can be improved by sintering the bulk at relatively high temperatures, which enables further diffusion, leading to more complete solid-state reactions that give a chemically homogeneous product [8]. In the case of a thick film the temperatures of synthesis and sintering are in the same range. Therefore, a special powder-synthesis method should be used to obtain a product that is as chemically homogeneous as possible. In our previous work a synthesis based on mechanochemical activation was used to obtain chemically homogeneous, fine-particle PMN–PT powder.

Due to its applicability in various fields, functional inkjet printing has drawn a lot of attention in recent years, e.g. printed circuit boards [9]. Conductors, resistors, capacitors and inductivities have been realized [10, 11, 12]. First attempts using inkjet printing for vertical interconnections have been taken by showing the feasibility of through silicon vias [13]. These applications demonstrate the

opportunities of inkjet printing with its high flexibility and scalability.

Flexibility, compared to screen printing, arises from several facts, namely contactless deposition, omission of screens/masks and applicability of in-situ blending.

For the combination of the promising PMN–PT characteristics and the advantages of inkjet printing, a corresponding ink has to be developed. This paper covers ink development as well as measurements on first printed layers.

## Materials & methods

### *Substrate preparation*

The 3 mm thick alumina substrates are prepared by slip casting from Alcoa A-16 and sintering at 1600 °C for 4 hours. A platinum paste (Ferro 6412), which is used as a bottom electrode, is screen printed and fired at 1200 °C for one hour on the Al<sub>2</sub>O<sub>3</sub> substrate. The thickness of the bottom electrode is around 10 μm.

### *PMN–PT powder preparation*

The starting compounds for the synthesis of the 0.65PMN–0.35PT material are PbO (99.9 %, Aldrich), MgO (98 %, Aldrich), TiO<sub>2</sub> (99.8 %, Alfa Aesar) and Nb<sub>2</sub>O<sub>5</sub> (99.9 %, Aldrich). A mixture of these oxides in the molar ratio corresponding to the stoichiometry of 0.65Pb(Mg<sub>1/3</sub>Nb<sub>2/3</sub>)O<sub>3</sub>–0.35PbTiO<sub>3</sub> (0.65PMN–0.35PT) with an excess of 2 mol% PbO is high-energy milled in a planetary mill (Retsch, Model PM 400). An excess amount of PbO is added for two reasons: to promote the sintering with the formation of a liquid phase rich in PbO and to replace the PbO lost from the PMN–PT during sintering. After the mechanochemical activation, the powder is milled in an attritor mill at 800 rpm for 4 hours in isopropanol, and then dried and sieved. The powder is then heated at 700 °C for 1 hour.

The size of the particles prepared by the mechanochemical activation was determined using a light-scattering technique. The particle size distribution is narrow with a median particle size  $d_{50}$  equal to 0.32 μm.

### *Ink preparation*

Initially, the PMN–PT powder has to be dispersed to a high-viscous paste which can later be thinned to a low-viscous ink. The paste allows long time stable storage without the risk of sedimentation or agglomeration. Additionally high shear forces can be applied to the paste, which allows for a high-grade dispersion.

To create the paste, PMN–PT powder is manually mixed with a small amount of glass frit and diethylene glycol monobutyl ether (BC). The mixture

is then treated in a three roll mill. BC is used to form a suspension with the PMN–PT particles and the glass frit. Ethyl cellulose encloses the particles, which leads to a lower virtual density of the single particles. This drastically reduces sedimentation after thinning the paste to an ink with a viscosity suitable for printing. Sedimentation is decreased further as ethyl cellulose prevents agglomeration due to steric stabilization. Adding the glass frit should improve particle adhesion on the substrate after sintering.

While ink viscosity and particle size are critical factors for the generation of drops with the printhead, their influence on flow behavior on the substrate is negligible. The main influence on flow behavior results from the interaction between substrate and solvent, respectively the wetting behaviour. Using a KRÜSS DSA 100 drop shape analysis system it is found that BC spreads on the platinum electrodes (i.e. the contact angle on the substrate is below 5°).

Usually, ink spreading on a substrate hinders fine homogeneous structuring. The next section introduces a two step printing process for printing smooth PMN–PT layers under the given conditions.

### *Printing process & sintering*

A single nozzle printhead MD-K-140 (microdrop Technologies GmbH, Germany) is used for printing. It is integrated in a self-developed printing station which comprises an ink reservoir, an underpressure/electrical control system and a heatable substrate table. Positioning accuracy of the table is 1 μm in x- and y-direction.

Optimum printing parameters (piezo voltage, pulse length and nozzle temperature) are determined and maintained by the printhead control system. For adjustment emitted drops are observed with a camera and stroboscope diode setup, which is triggered in coherence with the piezo voltage pulse.

A specifically designed LabView program controls the substrate table movement and the nozzle triggering. Monochrome bitmaps are used as printing layouts. Printing resolution (μm per pixel) is freely scalable in 1 μm steps, only limited by the substrate table's accuracy.

Multiple PMN–PT layers are printed. Successive layers are applied after the previous layer dried completely. Fast drying is achieved by heating the substrate table to 80 °C and by applying a hot airflow over the substrate. In addition to the heating, the airflow provides unsaturated air above the drying layer, thus, accelerating the process.

In the short waiting time (approximately 20 s) between printing of two layers the nozzle might clog. Clogging is avoided by continuously depositing drops next to the substrate while waiting. This enables printing for many hours without any ink stirring/circulation.

As mentioned above, the ink/substrate combination seems unfavorable for conventional multilayer inkjet printing due to the very low contact angle. Frayed edges can be seen after printing the films. At those edges, some coffee ring effect can be detected as well as the strongly non-circular shape of the spots.

Accordingly, first results for conventionally stacked layers show very inhomogeneous layer thickness. The LabView program is updated to overcome this. Every second layer is now printed with a shift of half of the resolution along  $x$ - and  $y$ -axis.

After printing and sintering at 950 °C for 2 h, the samples are ready for characterization.

### Characterization methods

First impressions concerning the printing results are obtained using a Keyence VHX-1000 optical microscope.

The piezoresponse of films is studied by AFM (Asylum Research) equipped with a piezoelectric module (PFM) in single frequency mode by application of an electric field with the amplitude of 20 V. Commercial silicon tips coated by conductive Ti/Ir layers with a force constant of 2 N/m and a resonance frequency of the lever of 70 kHz are used. The piezoelectric coefficients are determined at frequencies far away from the resonance frequency of the tip-sample system.

## Results & discussion

### Ink properties

When it comes to inkjet printing, a low viscosity ink has to be provided. The nozzle used in these trials (70  $\mu\text{m}$  nozzle diameter) requires a viscosity lower than 12 mPas. Based on the previous paste, this viscosity can be met in multiple ways.

First, by thinning and, second, by heating the thinned ink. The lower limit of the viscosity achievable by thinning is given by the viscosity of BC which is about 6 mPas at room temperature. However, excessive thinning comes along with an extremely low solid substance content and faster sedimentation. Thus, it is advisable to increase ink temperature, which results in a significant viscosity drop. At 30 °C target viscosity of 9 mPas (shear rate 1000  $\text{s}^{-1}$ , corresponding to printing conditions in the nozzle) is reached at a solid substance content of 18.5 wt%, i.e. approx. 10 vol%. The solid substance content in vol% is estimated after density measurements (DMA-4500, Anton Paar). Ink density is 1.13  $\text{g}\cdot\text{cm}^{-3}$ . However, we found that drop formation shows best results at 55 °C, where ink viscosity is even lower (**Figure 1**).

This temperature is favorable when printing for two reasons. First, it can easily be controlled, second, it is still low enough to prevent nozzle clogging.

Applying these parameters, a drop with a diameter of 67  $\mu\text{m}$  is ejected from the nozzle.

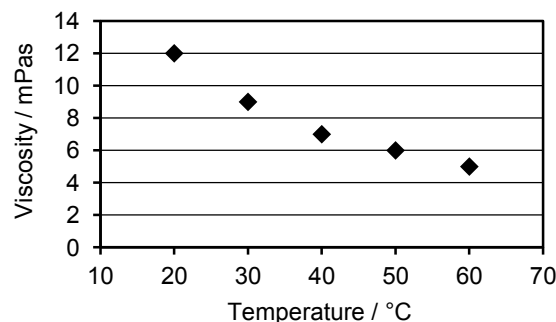


**Figure 1.** Ink viscosity at temperatures from 20 °C to 60 °C measured at a shear rate of 1000  $\text{s}^{-1}$ .

### Conventionally stacked layers

Inkjet-films printed in a conventional multilayer process show a bumpy structure when printed with drop spacing of 150  $\mu\text{m}$  for 30 layers (**Figure 2**). High layer thickness is found where drops are placed. Between the single spots, layer thickness is very low. Sintering even leads to cracking respectively gapping of the inhomogeneous PMN-PT surface due to shrinkage.

When increasing the number of layers to 50, even larger gaps appear (**Figure 3**). Eventually, with increasing film thickness parts of it start peeling off of the substrate in addition to gap appearance. This occurs for the film printed with 100 layers shown in **Figure 4**, though peel off can barely be seen under the microscope. When reaching higher thickness (200 layers), no gaps appear. Instead, massive peel off occurs due to strong sintering shrinkage and especially due to low adhesion on the substrate (**Figure 5**).

An usual approach to overcome these inhomogeneities and gap formation is a reduction of drop spacing. In this case, however, it leads to inhomogeneous layers as well, as a very large amount of ink is deposited at the same time causing an extensive particle flow on the substrate surface. The solution is the introduction of shifted stacked layers as described before. Results for these films are discussed in the next section.

In spite of gaps and partial peel off, the presence of the piezoelectric behavior is proven by PFM. The local piezoelectric coefficient  $d_{33}$  ranges from 1-2 pm/V for the 50 layers samples (**Figure 3**) over 4 pm/V for 30 layers samples (**Figure 2**) to 6 pm/V for 100 layers samples (**Figure 4**). Different values of  $d_{33}$  presumably result from film inhomogeneities and defects, however all the values are of the same order of magnitude.

The achieved values of  $d_{33}$  are low in comparison with bulk ceramics of the same composition [2] or thick films prepared by screen-printing ( $d_{33} > 150$  pm/V [14, 15]).

However, these first trials demonstrate the presence of a piezoelectric response in inkjet printed films.

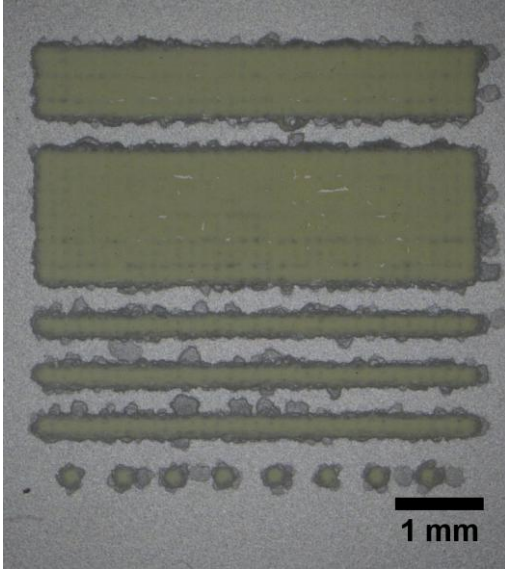


**Figure 2.** Conventional multilayer films, lines and dots after sintering. Small cracks for 30 layers printed.

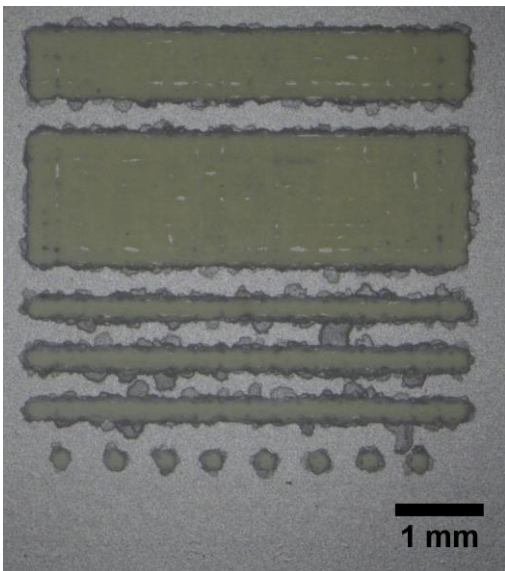


**Figure 3.** Conventional multilayer films, lines and dots after sintering. More and larger cracks for 50 layers printed.

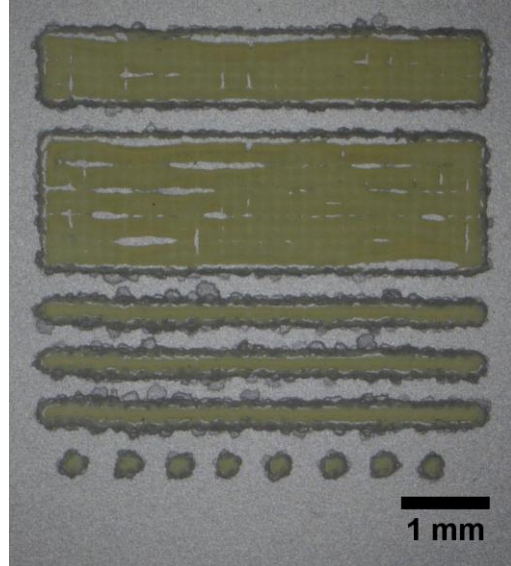


**Figure 4.** Conventional multilayer films, lines and dots after sintering. Massive cracks and partial peel off for 100 layers printed.

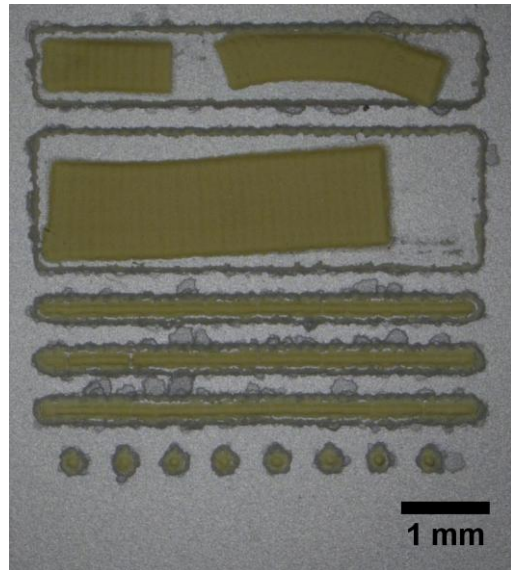


**Figure 5.** Conventional multilayer films, lines and dots after sintering. Excessive peel off caused by sintering shrinkage for 200 layers printed.

### Shifted stacked layers

Printing every second layer with a shift of half the pitch, i.e. 75  $\mu\text{m}$ , along  $x$ - and  $y$ -axis leads to a smoother, more homogeneous surface. By eliminating inhomogeneities the occurrence of gaps and peel off are avoided (**Figure 6**).

For homogeneous films with length  $l$  and width  $w$ , layer thickness  $h$  can be calculated. The total amount of deposited solid substance is estimated from the number of drops deposited  $n$  and the volume of their solid substance  $V_{ss}$ . Layer thickness then is

$$h = \frac{n \cdot V_{ss}}{l \cdot w}. \quad (1)$$

This leads to a thickness of 23.5  $\mu\text{m}$  and 47  $\mu\text{m}$  for 20 and 40 printed layers, respectively.

Both of the films show piezoelectric behavior, however, the response is still very low. The local piezoelectric coefficient  $d_{33}$  is of the same order of magnitude as for films shown in **Figures 2 – 5** (i.e.  $d_{33}$  of 2 pm/V for both films in **Figure 6**).

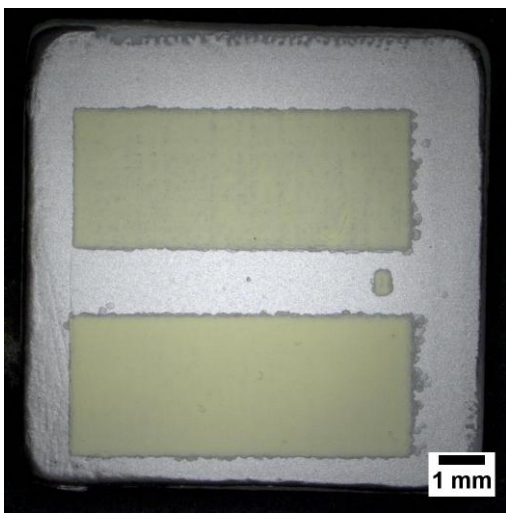


**Figure 6.** Shifted stacked layers after sintering. The top film consists of 20 layers, the bottom film of 40 layers.

### Conclusions & Outlook

In this work, a PMN–PT ink is developed and used for inkjet printing of PMN–PT thick films for the first time. Films are prepared by inkjet printing of PMN–PT ink on platinumized  $\text{Al}_2\text{O}_3$  substrates and subsequent firing at 950  $^\circ\text{C}$  for 2 h.

Preparation of three different shapes is shown in this work. First, dots consisting of stacked single drops, second, lines formed from neighboring drops and, third, rectangular shapes. Rectangular shapes are printed in a shifted stacked layer design, where every second layer is printed with a shift of half the pitch. This unconventional printing process provides homogeneous layer thickness not achievable by conventional layer stacking using this ink/substrate combination.

The piezoelectric coefficient  $d_{33}$  of inkjet printed PMN–PT films is low in comparison with bulk ceramics or thick films prepared by screen printing method. However, the presence of piezoelectric response in inkjet printed PMN–PT films is demonstrated. Further improvements, especially in ink composition, but also in printing and sintering will need to be applied to obtain even better piezoelectric performance of the films.

### Acknowledgements

The authors would like thank S. Drnovšek and D. Žehelj from JSI for their help with the experimental work. H. Uršič thanks the Slovenian Research Agency for financial support (P2-0105, J2-3633).

### References

- [1] J. Kelly, M. Leonard, C. Tantigate, A. Safari, “Effect of composition on the electromechanical properties of  $(1-x)\text{Pb}(\text{Mg}_{1/3}\text{Nb}_{2/3})\text{O}_3-x\text{PbTiO}_3$  ceramics”, *J. Am. Ceram. Soc.*, vol. 80, pp. 957–964, 1997.
- [2] H. Uršič, J. Tellier, M. Hrovat, J. Holc, S. Drnovšek, V. Bobnar, M. Alguero, M. Kosec, “The effect of poling on the properties of  $0.65\text{Pb}(\text{Mg}_{1/3}\text{Nb}_{2/3})\text{O}_3-0.35\text{PbTiO}_3$  ceramics”, *Jap. J. Appl. Phys.*, vol. 50, pp. 035801–035806, 2011.
- [3] O. Noblanc, P. Gaucher, G. Calvarin, “Structural and dielectric studies of  $\text{Pb}(\text{Mg}_{1/3}\text{Nb}_{2/3})\text{O}_3-\text{PbTiO}_3$  ferroelectric solid solutions around the morphotropic boundary”, *J. Appl. Phys.*, vol. 79, pp. 4291–4298, 1996.
- [4] K. Uchino, S. Nomura, L. E. Cross, S. E. Jang, R. E. Newnham, “Electrostrictive effect in lead magnesium niobate single crystals”, *J. Appl. Phys.*, vol. 51, pp. 1142–1146, 1980.
- [5] J. Zhao, Q. M. Zhang, N. Kim, T. Shrout, “Electromechanical properties of relaxorferroelectric lead magnesium niobate-lead titanate ceramics”, *Jap. J. Appl. Phys.*, vol. 34, pp. 5658–5663, 1995.
- [6] H. Uršič, M. Škarabot, M. Hrovat, J. Holc, M. Skalar, V. Bobnar, M. Kosec, I. Mušević, “The electrostrictive effect in ferroelectric  $0.65\text{Pb}(\text{Mg}_{1/3}\text{Nb}_{2/3})\text{O}_3-0.35\text{PbTiO}_3$  thick films”, *J. Appl. Phys.*, vol. 103, pp. 124101–124101, 2008.
- [7] G. H. Haertling, “Ferroelectric Ceramics: History and Technology”. *J. Am. Ceram. Soc.*, vol. 82, pp. 797–818, 1999.
- [8] S. Bernik, R. B. Marinenko, J. Holc, Z. Samardžija, M. Čeh and M. Kosec, “Compositional homogeneity of ferroelectric  $(\text{Pb},\text{La})(\text{Ti},\text{Zr})\text{O}_3$  thick films”, *Material Research Society*, vol. 18, pp. 515, 2003.
- [9] T. Sutter, “An overview of digital printing for advanced interconnect applications”, *Circuit World*, Vol. 31, No. 3, pp. 4–9, 2005.

- [10] D. Jeschke, E. Ahls, K. Krueger, "Inkjet-Printing of Multilayer Capacitors", *Journal of Microelectronics and Electronic Packaging*, Vol. 9, No. 3, pp. 126-133, 2012.
- [11] M. Wassmer, W. Diel, K. Krueger, "Inkjet Printing of Fine-Line Thick-Film Inductors", *Journal of Microelectronics and Electronic Packaging*, Vol. 7, No. 4, 2010.
- [12] B. J. Kang, C. K. Lee, J. H. Oh, "All-inkjet-printed electrical components and circuit fabrication on a plastic substrate", *Microelectronic Engineering*, Vol. 97, pp. 251-254, 2012.
- [13] A. Rathjen, Y. Bergmann, K. Krueger, "Feasibility Study: Inkjet Filling of Through Silicon Vias (TSV)", *NIP28: International conference on Digital Printing Technologies and Digital Fabrication*, pp. 456-460, 2012.
- [14] H. Uršič, M. Santo Zarnik, J. Tellier, M. Hrovat, J. Holc, M. Kosec, "The influence of thermal stresses on the phase composition of 0.65Pb(Mg<sub>1/3</sub>Nb<sub>2/3</sub>)O<sub>3</sub>-0.35PbTiO<sub>3</sub> thick films", *J. Appl. Phys.*, Vol. 109, pp. 01410, 2011.
- [15] M. Kosec, H. Uršič, J. Holc, M. Hrovat, D. Kuščer, B. Malič, "High-Performance PMN-PT Thick Films", *IEEE Ultrasonics, Ferroelectrics and Frequency Control*, Vol. 57, No. 10, pp. 2205-2212, 2010.